Electronic Supplementary Information

A Biomarker-responsive Nanoprobe for Detecting Hepatic Ischemia-reperfusion Injury via Optoacoustic/NIR-II Fluorescence Imaging

Zhuo Zeng, Junjie Chen, Lihe Sun, Fang Zeng* and Shuizhu Wu*
State Key Laboratory of Luminescent Materials and Devices, Guangdong Provincial Key Laboratory of Luminescence from Molecular Aggregates, College of Materials Science and Engineering, South China University of Technology, Guangzhou 510640, China

[*] Corresponding authors
E-mail: mcfzeng@scut.edu.cn
shzhwu@scut.edu.cn

Table of contents

Experimental section

1. Reagents.

2,3-Dichloro-5,6-dicyano-1,4-benzoquinone, boron trifluoride diethyl etherate, trifluoroacetic acid, triethylamine, phosphorus tribromide (PBr_3), cyclohexanone and acetic acid were purchased from Energy Chemical Reagents Ltd.. Cesium carbonate (Cs_2CO_3), 8-hydroxyjulolidine-9-carboxaldehyde, 4-pyridinecarboxaldehyde, 4-(bromomethyl) phenylboronic acid and 2,4-dimethylpyrrole were purchased from Bide Pharmaceutical Technology Co., Ltd.. The solvents including dichloromethane (DCM) and N, N-dimethylformamide (DMF) of analytical grade were dried with molecular sieves. Other solvents used in this study were analytical grade reagents without further purification. The water used in the experiments was the triple-distilled water.

2. Apparatus.

Nuclear magnetic resonance (NMR) spectra were measured on Bruker AVANCE 500 MHz NMR spectrometer. ^{1}H NMR was conducted at 500 MHz. High resolution mass spectrometer (HR-MS) was recorded on a Bruker MAXIS IMPACT mass spectrometer. High performance liquid chromatography (HPLC) measurements were carried out on Agilent high performance liquid chromatograph 1260 Infinity (with DAD). The Near-Infrared-II (NIR-II) fluorescence spectra were obtained on NIRQUEST512 spectrometer (excitation: 808 nm laser, emission range: 900-1700 nm). The absorption spectra were collected on Hitachi U-3010 absorption spectrophotometer. The NIR-II fluorescence (in vivo and ex vivo) imaging was conducted on NIR-II in-vivo Fluorescent Imaging System (Series II 808/900-1700, Suzhou NIR-Optics Technologies Co., Ltd.). Optoacoustic imaging was performed using inVision128 multispectral optoacoustic tomographic (MSOT) imaging system (iThera Medical GmbH) equipped with viewMSOT 4.0 for data processing.

3. Syntheses.

Synthesis of BOD:

Compound BOD was prepared as described previously [1].

Synthesis of A:

Compound A was prepared as described previously [2].

Synthesis of XJ:

8-Hydroxyjulolidine-9-carboxaldehyde (0.6 g, 2.76 mmol) and Cs_2CO_3 (2.63 g, 8.06 mmol) were dissolved in 15 mL anhydrous DMF in a 50 mL round-bottomed flask. Compound A (1.07 g, 5.61 mmol) was dissolved in 2 mL anhydrous DMF and subsequently injected into the flask. The mixture was stirred at room temperature for 48 hours. Afterward, the resulting mixture was filtered, and the filtrate was concentrated under reduced pressure. Then the mixture was washed three times with water and extracted with ethyl acetate. The combined organic layers were dried with anhydrous Na_2SO_4 and evaporated under reduced pressure. The residue was purified using silica gel chromatography petroleum ether/ethyl acetate (7:1, v/v) as eluent to obtain compound XJ as orange powder. Yield: 170 mg (20 %). ^{1}H NMR (500 MHz, $CDCl_3$, Fig. S1) δ 10.19 (s, 1H), 6.55 (s, 1H), 6.51 (s, 1H), 3.12-3.15 (m, 4H), 2.72 (t, *J* = 6.6 Hz, 2H), 2.64 (t, *J* = 6.2 Hz, 2H), 2.46 (t, *J* = 6.1 Hz, 2H), 2.38 (t, *J* = 6.0 Hz, 2H), 1.87-1.92 (m, 4H), 1.60 – 1.65 (m, 2H). HR-MS (ESI) (m/z, Fig. S2) $[M+H]^+$ calcd for $[C_{20}H_{22}NO_2]^+$: 308.1651, found 308.1645.

Synthesis of BX:

Compound BOD (325 mg, 1 mmol) and compound XJ (462 mg, 1.5 mmol), glacial acetic acid (0.2 mL) and piperidine (0.25 mL) were dissolved in methylbenzene (10 mL). The mixture was stirred at 110 ℃ for 8 h. Any water formed during the reaction was removed azeotropically in a dean-stark apparatus. The solvent was evaporated and the crude product was purified by column chromatography dichloromethane/ethyl acetate (25:1, v/v) to afford the blue-green solid product. Yield: 92 mg (15 %). ^{1}H NMR (500 MHz, $CDCl_3$, Fig. S3) δ 8.76 (d, *J* = 4.9 Hz, 2H), 7.54 (d, *J* = 8.4 Hz, 2H), 7.35 (d, *J* = 1.9 Hz, 1H), 7.34 (s, 1H), 7.28 (d, *J* = 2.1 Hz, 1H), 7.14 (d, *J* = 2.5 Hz, 1H), 7.12 (d, *J* = 2.5 Hz, 1H), 6.98 (s, 1H), 2.84 (t, *J* = 8.1 Hz, 2H), 2.59 (dd, *J* = 15.0, 7.5 Hz, 2H), 2.35 (t, *J* = 7.5 Hz, 2H), 2.04 (t, *J* = 2.1 Hz, 2H), 2.01 (d, *J* = 5.5 Hz, 4H), 1.69-1.64 (m, 4H), 1.59 (s, 9H), 1.50-1.46 (m, 2H). HR-MS (ESI) (m/z, Fig. S4) $[M]^+$ calcd for $[C_{38}H_{37}BF_2N_4O]^+$: 614.3028, found 614.3030.

Synthesis of Synthesis of BX-BOH:

Compound BX (381 mg, 0.62 mmol) and 4-(bromomethyl) phenylboronic acid (1077 mg, 5.01 mmol) were dissolved in dry ACN (10 mL). Then, the mixture was stirred at 85 ℃ for 12

h. The solvent was evaporated and the crude product was purified by column chromatography (dichloromethane/methanol = 50:1) to afford the green solid product. Yield: 116 mg (25 %). ^{1}H NMR (500 MHz, DMSO-d_6) δ 9.38 (d, J = 12.4 Hz, 2H), 8.48 (d, J = 17.1 Hz, 2H), 7.72 (d, J = 8.1 Hz, 2H), 7.62 (d, J = 8.4 Hz, 2H), 7.57 (d, J = 7.6 Hz, 1H), 7.42 (d, J = 3.0 Hz, 1H), 7.40 (s, 1H), 7.29 (d, J = 6.7 Hz, 1H), 7.20 (s, 1H), 6.89 (s, 1H), 6.01 (s, 2H), 2.99 (d, J = 20.3 Hz, 2H), 2.91 (d, J = 14.3 Hz, 2H), 2.69 – 2.73 (m, 2H), 2.63(d, J =8.4 Hz, 2H), 2.41 (d, J = 6.5 Hz, 2H), 2.32 (s, 2H), 1.99 (s, 9H), 1.86-1.91 (m, 4H), 1.43 – 1.47 (m, 2H). $[M]^+$ calcd for $[C_{45}H_{45}B_2F_2N_4O_3]^+$: 749.3646, found 749.3628.

4. Preparation of the BX-BOH@BSA nanoparticle and measurement of absorption and fluorescence spectra

The probe BX-BOH's stock solution (1 mM) was prepared in DMSO. Afterward, the stock solution was added dropwise into the phosphate-buffered saline (PBS) (pH 7.4, 10 mM), which contained BSA (BSA: 30 mg mL^{-1}). After that, this mixture solution was vortexed for 30 min to form the nanoparticle BX-BOH@BSA. The nanoprobe BX-BOH@BSA was freshly prepared for use.

The optical response of the nanoprobe BX-BOH@BSA towards H_2O_2 was carried out according to the following procedures. H_2O_2 was added to BX-BOH@BSA solution (final BX-BOH@BSA concentration: 0.6 mg mL^{-1}, H_2O_2 concentration: 0 to 90 μM, in PBS (pH 7.4, 5% DMSO)). After the addition of H_2O_2, the reaction solutions were kept at 37 ℃ for 0 - 80 min, and their absorption and NIR-II fluorescence spectra were measured. The NIR-II fluorescence emission spectra were measured with an 808 nm laser at a power density of 50 mW cm^{-2}.

5. Cell experiments.

L929 cells were provided KeyGEN BioTECH Co., Ltd. and cultured in Dulbecco's modified Eagle's medium (DMEM) containing 10% (v/v) fetal bovine serum. Cell incubator was maintained at 37 ℃ and a humidified 5% CO_2 atmosphere. The cytotoxicity of BX-

BOH@BSA was evaluated on L929 cells by standard methyl thiazolyl tetrazolium (MTT) assay. Briefly, cells were seeded into 96-well plates at a cell density of 5000 cells per well and cultured for 24 h. Then, the medium in all wells was replaced with fresh one containing different concentrations of the nanoprobe (0, 0.15, 0.3, 0.6, 1.8 and 3.6 mg mL^{-1}), and the cells were cultured for another 24 h. After that, MTT salts (0.5 mg mL^{-1}) was added to the culture medium in each well and incubated for an additional 4 h. Finally, each well was washed with sterile PBS for 3 times and the medium was replaced with 150 μL DMSO to dissolve the precipitates. The optical density at 570 nm for each well was measured by Thermo MK3 ELISA reader to access cell viability. Three independent experiments were conducted for each concentration and 8 replicates were performed in each independent experiment.

6. Animal experiments.

Animal experiments were conducted in accordance with the approval by the Ethics Committee of Laboratory Animal Center of South China Agricultural University (SCAU-2022d109). Male BALB/c mice (5-6 weeks old) were purchased from Guangdong Medical Laboratory Animal Center and kept in a specific-pathogen-free (SPF) laboratory animal center of South China Agricultural University under standard care. Free access to SPF diet and sterile water were ensured for the mice which were kept at a 12/12 h light/dark cycle. In the experiments, mice were randomly assigned to five mice per group.

7. Mouse model of hepatic ischemia-reperfusion injury (HIRI)

The male BALB/C mice (5–6 weeks old) were randomly divided into four groups (n = 5 per group) as follows:

Sham group as the control: Namely healthy mice without undergoing ischemia and reperfusion processes.

I/R: 30min/24h group: The mice were given a midline laparotomy surgery, and ischemia was induced by clamping the hepatic artery and portal vein for 30 min followed by reperfusion for 24 h.

I/R: 60min/24h group: The mice were given a midline laparotomy surgery, and ischemia was induced by clamping the hepatic artery and portal vein for 60 min followed by reperfusion for 24 h.

NAC group (the therapy group): The mice were treated with an antioxidative drug N-acetylcysteine (NAC) (150 mg kg^{-1} body weight daily) for 2 days prior to the ischemia procedure for I/R: 60min/24 h group.

During the midline laparotomy surgery, the mice were anesthetized by inhaling 1% isoflurane, and the ischemia was performed using atraumatic vascular clamp. After 30 min or 60 min of ischemia, the clamp was removed, followed by suturing the abdominal cavity layer by layer (total reperfusion time: 24 h).

8. In vivo imaging for HIRI model mice

Mice were depilated with commercial depilatory cream before the imaging experiments. For NIR-II fluorescent imaging, 808 nm laser was used as the excitation light with a power density of 50 mW cm^{-2} on the imaging plane. Optoacoustic (OA) imaging was conducted on the inVision 128 MSOT system from iThera Medical GmbH, and the data processing software was viewMSOT 4.0.

For the purpose of detection, imaging experiments including NIR-II fluorescent imaging and MSOT imaging were performed after the establishment of the HIRI model. Before imaging, mice from different groups were given an intravenous injection of 4.0 mg kg^{-1} BX-BOH@BSA and imaged at predetermined time intervals (0, 30 and 90 min).

In MSOT imaging, 680, 700, 710, 720, 730, 745, 760, 780, 800, 850 and 900 nm were selected as the imaging wavelengths, considering the major turning points of the absorption of BX (the activated form of BX-BOH), Hb and HbO_2, and 10 frames per wavelength were recorded. Among them, 900 nm was chosen as the background wavelength to reflect the mouse anatomy. Cross-sectional images were acquired with a step size of 0.3 mm spanning through the whole liver region. With the aid of viewMSOT 4.0, these two-dimensional (2D) cross-sectional images were reconstructed to output the z-stack orthogonal-view three-dimensional (3D) images. Spectral unmixing was utilized to differentiate signal contribution from BX (the activated probe).

9. Mice weight assessment

Body weights for healthy mice i.v. injected with saline (the control) or the nanoprobe BX-BOH@BSA (4 mg kg^{-1}) daily for 7 days. Then, the body weight of the mice was measured daily for 7 days.

10. Tissue histological evaluation

For biosafety evaluation, the healthy mice were i.v. injected with the nanoprobe BX-BOH@BSA (4 mg kg^{-1}) or isovolumic saline daily. The mice were euthanized, so that the major organs (including hearts, livers, spleens, lungs and kidneys) were collected after 7 days. The organs's tissues were fixed with 10% paraffin and embedded in paraffin wax. After that, the embedded tissue samples were sectioned for hematoxylin and eosin (H&E) staining.

For the evaluation of HIRI, after reperfusion for 24 h, the mice in four different groups were euthanized and the liver was excised and subjected to histological analyses via H&E staining.

11. Serum biochemistry assessment

Serum ALT and AST levels were measured by Elisa Kits.

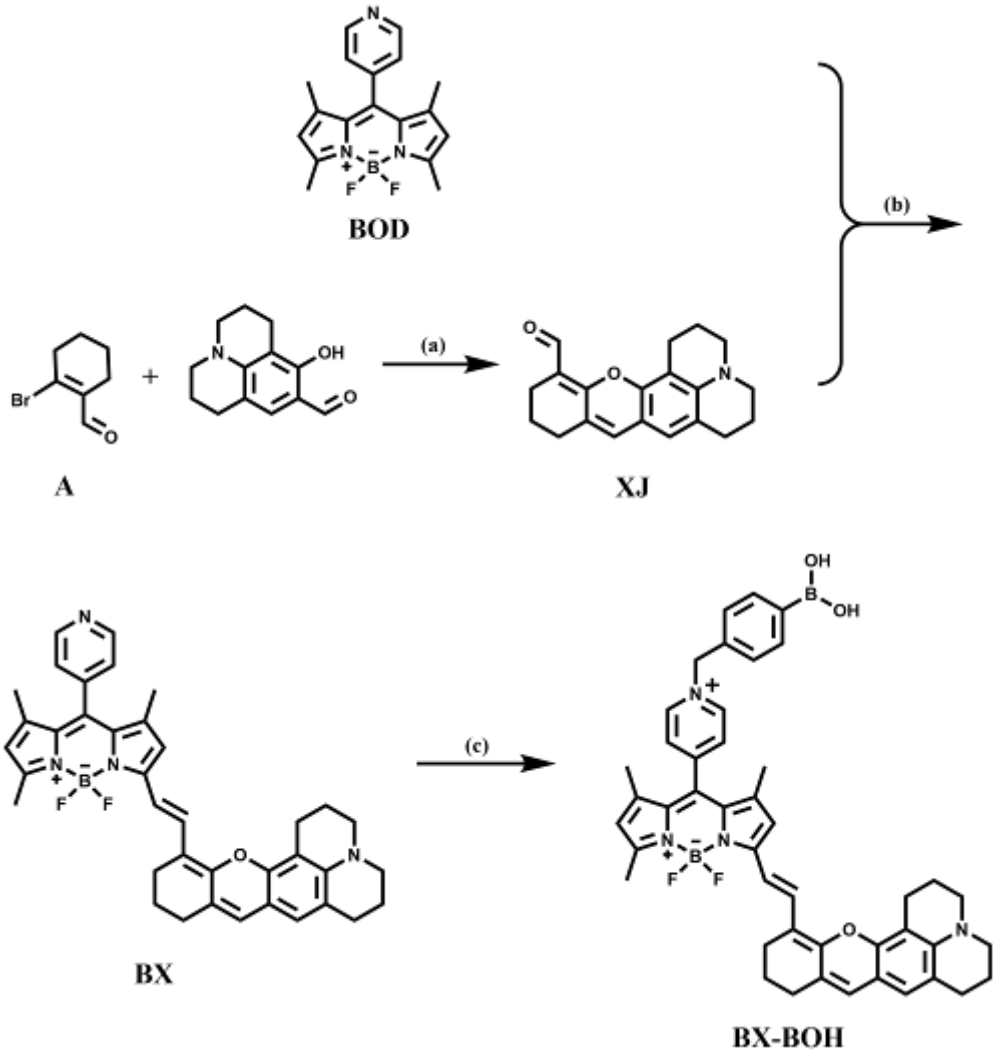

Scheme S1. Synthetic route for BX-BOH.

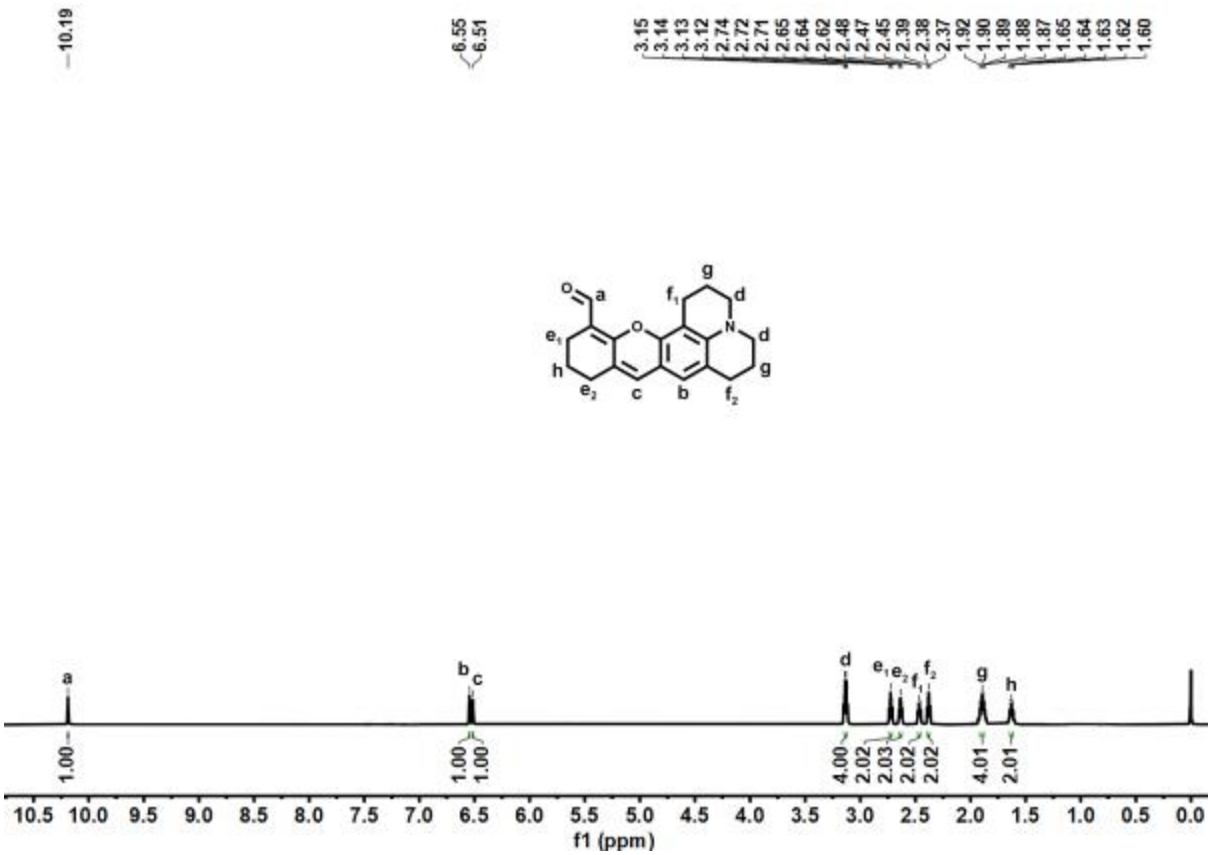

Fig. S1. ^{1}H NMR spectrum of XJ in $CDCl_3$.

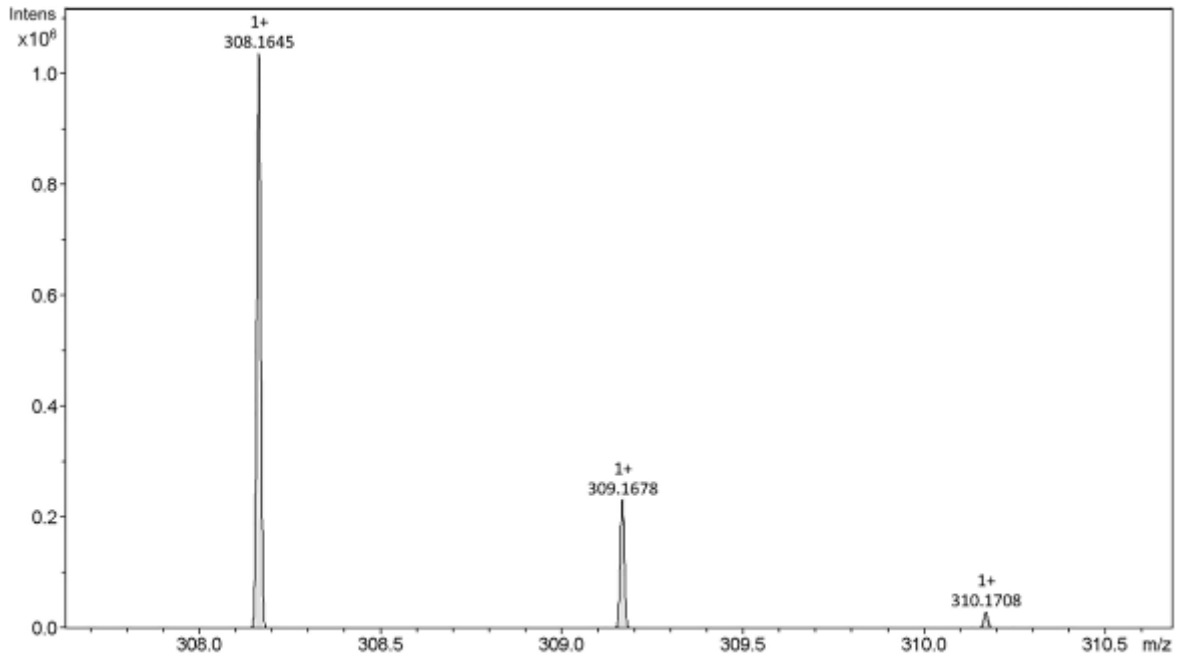

Fig. S2. HR Mass spectrum of XJ.
m/z $[M+H]^+$ $[C_{20}H_{22}NO_2]^+$ 308.1645

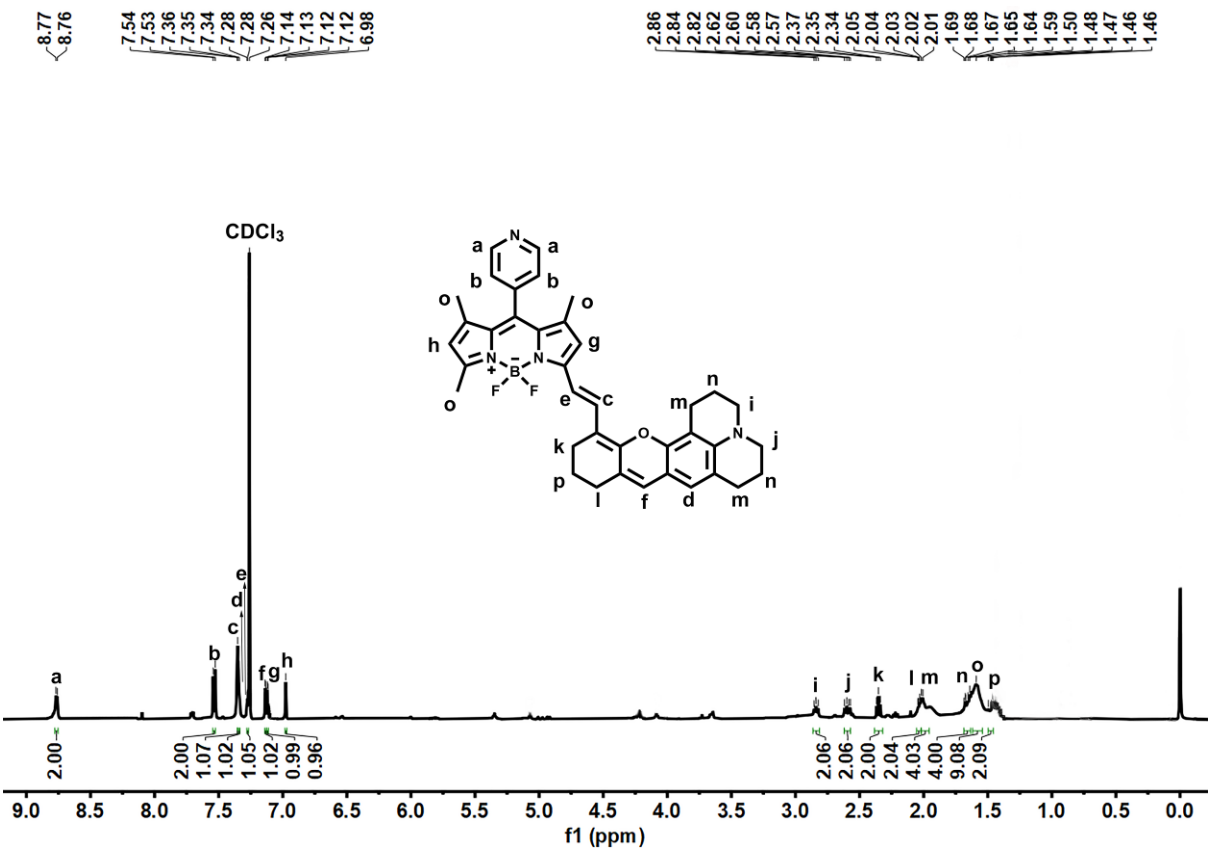

Fig. S3. ^{1}H NMR spectrum of BX in $CDCl_3$.

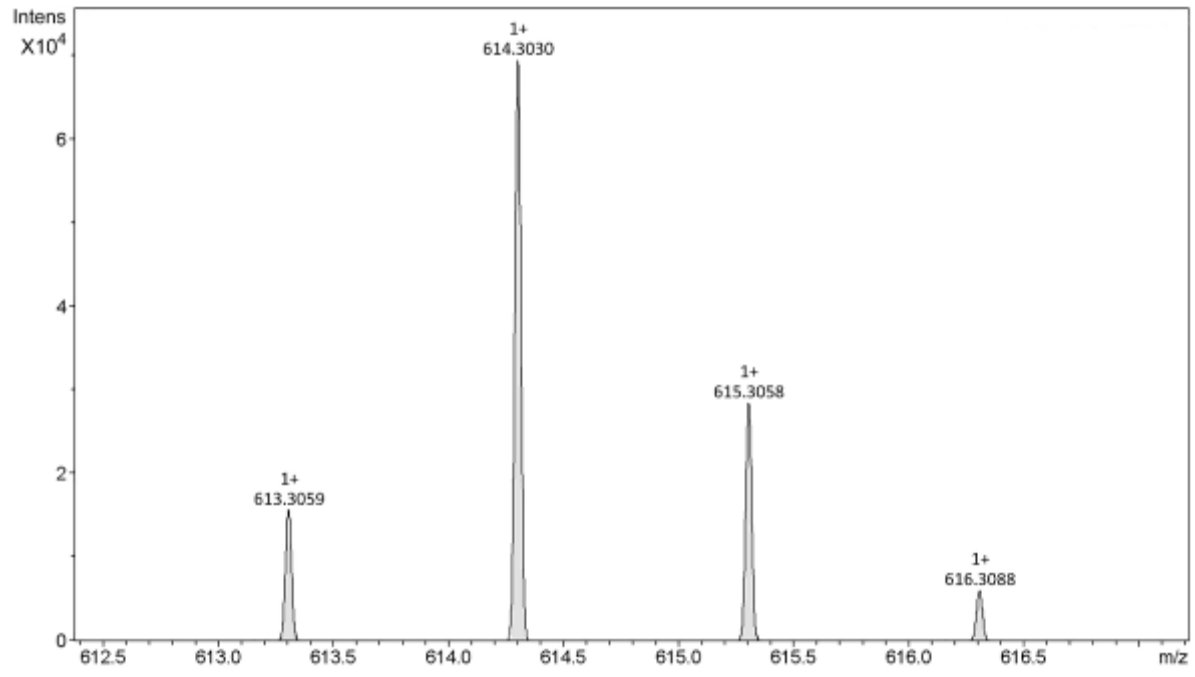

Fig. S4. HR Mass spectrum of BX.

m/z $[M]^+$ $[C_{38}H_{37}BF_2N_4O]^+$ 614.3030.

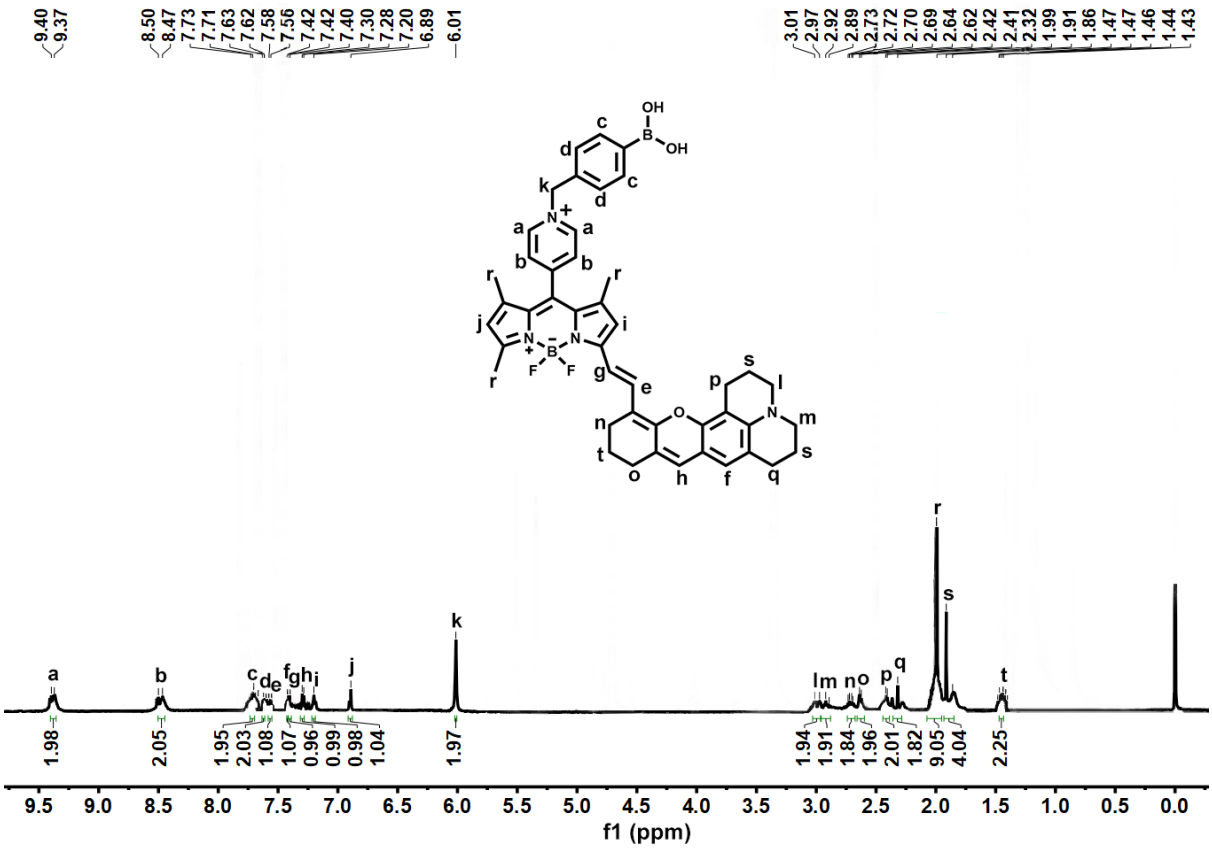

Fig. S5. ^{1}H NMR spectrum of BX-BOH in DMSO-d_6.

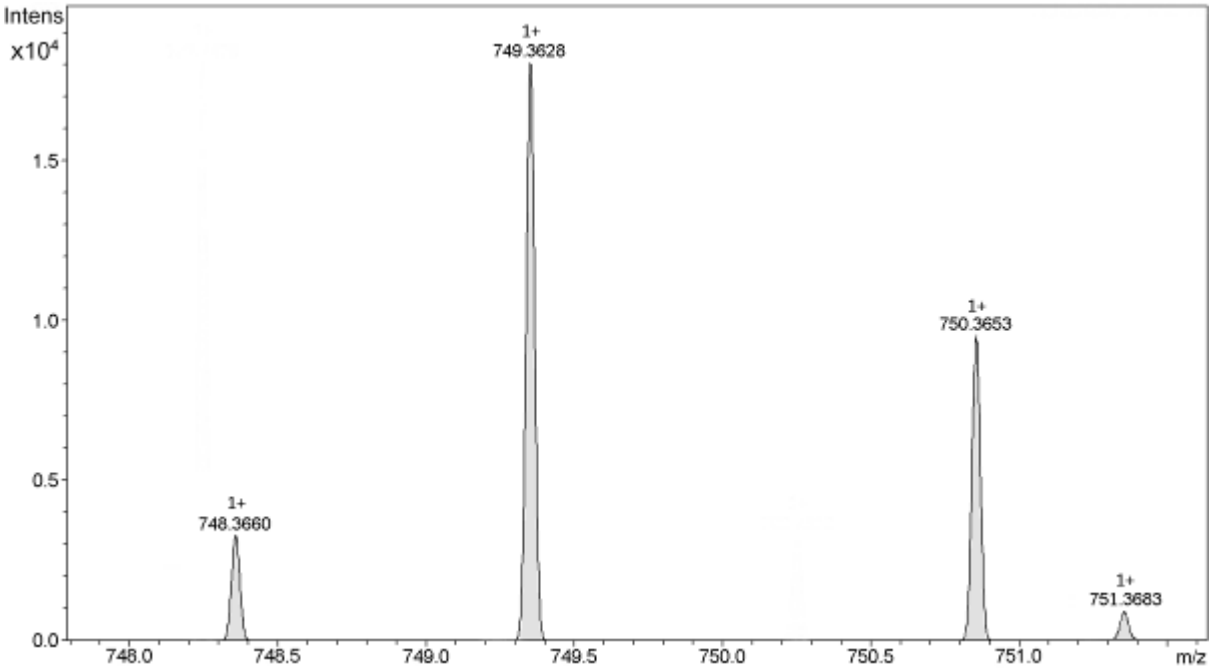

Fig. S6. HR Mass spectrum of BX-BOH.
m/z $[M]^+$ $[C_{45}H_{45}B_2F_2N_4O_3]^+$ 749.3628

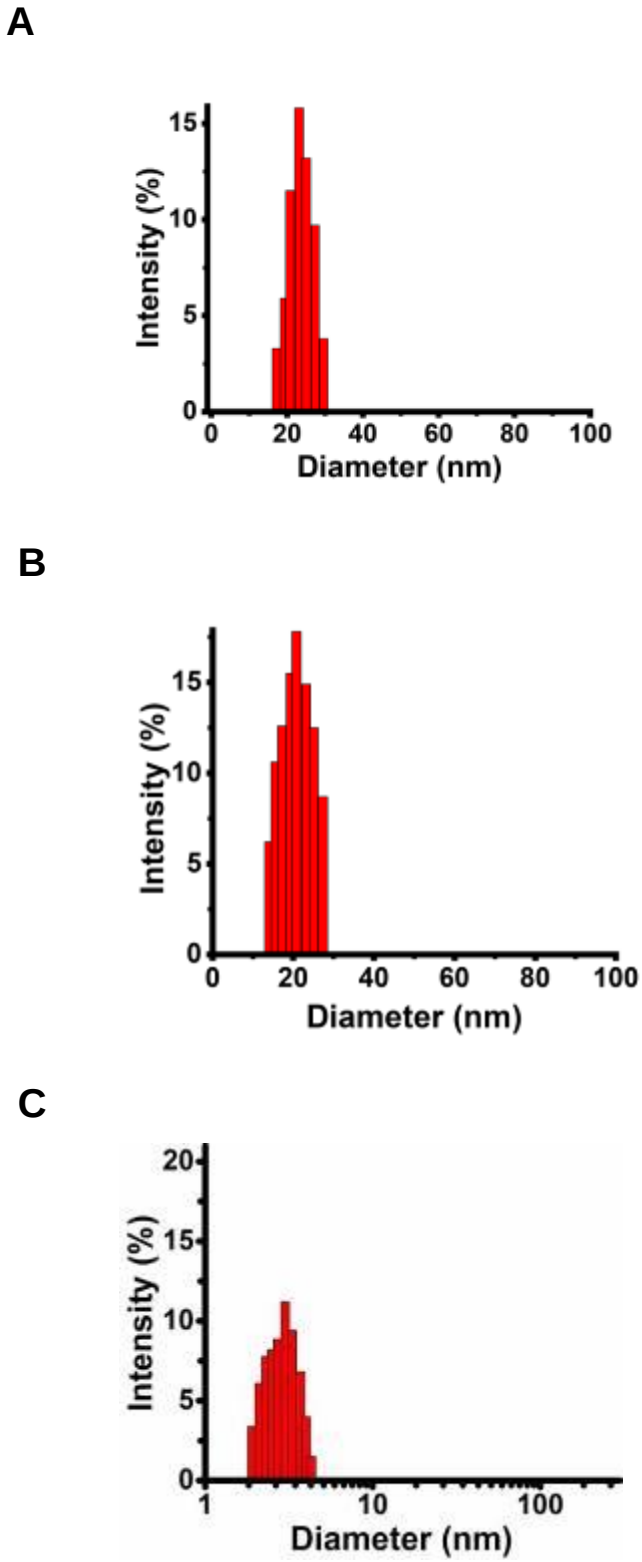

Fig. S7 Particle size distribution for BX-BOH@BSA in PBS containing 5% DMSO (A), BX@BSA in PBS containing 5% DMSO (B) and BX-BOH in PBS containing 20% DMSO (C) recorded by DLS.

BX-BOH directly precipitates in PBS containing 5% DMSO, since it is not water dispersible, hence its particle size distribution is measured in PBS containing 20% DMSO.

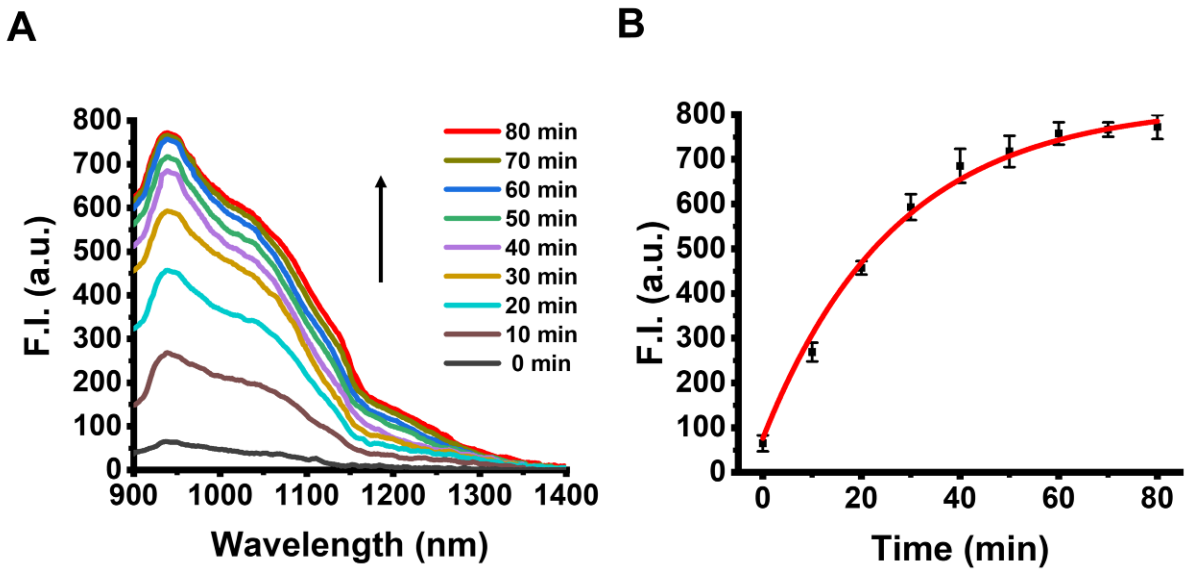

Fig. S8 (A) Time-dependent NIR-II fluorescence spectra of the nanoprobe BX-BOH@BSA (0.6 mg mL^{-1}) upon incubation with 90 μM H_2O_2 for varied time in PBS (pH 7.4, containing 5% DMSO). (B) Plot of fluorescence intensity (at 938 nm) versus incubation time for the nanoprobe BX-BOH@BSA after incubation with 90 μM H_2O_2. Data are means ± SD (n = 3). Excitation wavelength: 808 nm.

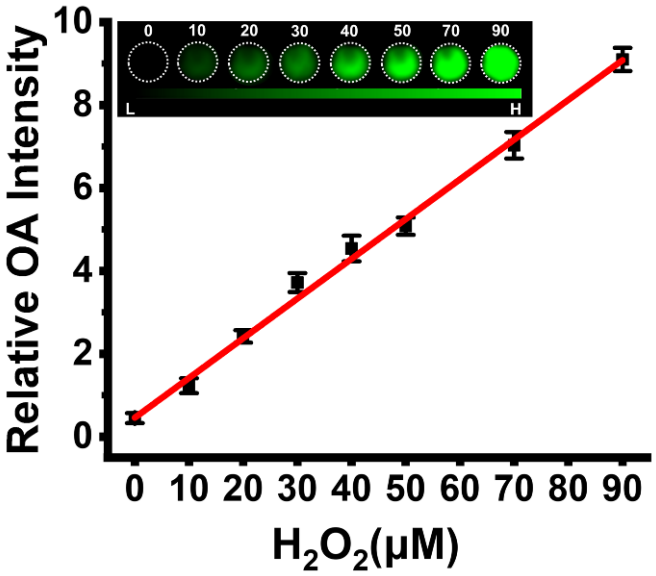

Fig. S9 Relative optoacoustic intensity at 740 nm for BX-BOH@BSA upon incubation with varied concentrations of H_2O_2 in PBS (with 5% DMSO, pH 7.4) (n=3). Inset: Representative optoacoustic images of BX-BOH@BSA treated with varied concentrations of H_2O_2.

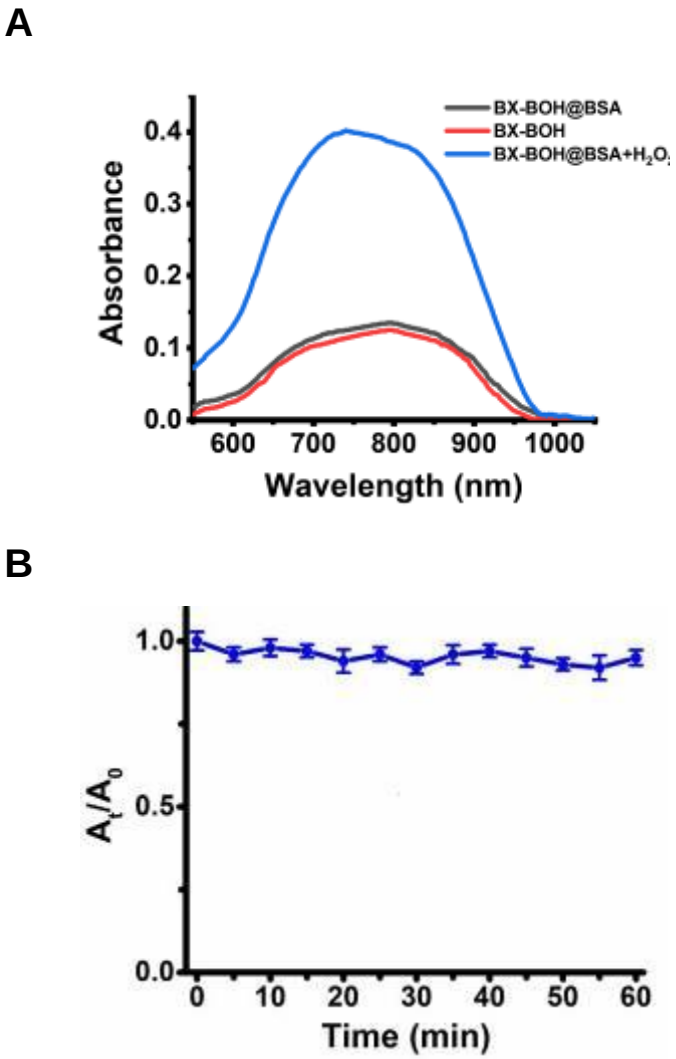

Fig. S10 (A) Absorption spectra for BX-BOH, the nanoprobe BX-BOH@BSA, the nanoprobe BX-BOH@BSA upon incubation with H_2O_2 (90 μM) in PBS (with 5% DMSO, pH 7.4). (B) Relative absorbance of BX-BOH (in PBS containing 20% DMSO) upon being irradiation by 808 nm laser. A_t represents the absorbance at time t, A_0 represents the absorbance before laser irradiation.

The stability of BX-BOH (in PBS containing 20% DMSO) has been evaluated by measuring the absorbance with continuous laser irradiation (808 nm, 50 mW cm^{-2}). It can be seen that the absorbance of the BX-BOH does not show obvious changes. The results suggest that BX-BOH is relatively stable under laser irradiation with ambient oxygen and is suitable for working under the normal imaging conditions.

BX-BOH directly precipitates in PBS containing 5% DMSO, since it is not water dispersible, hence the measurements were conducted in PBS containing 20% DMSO.

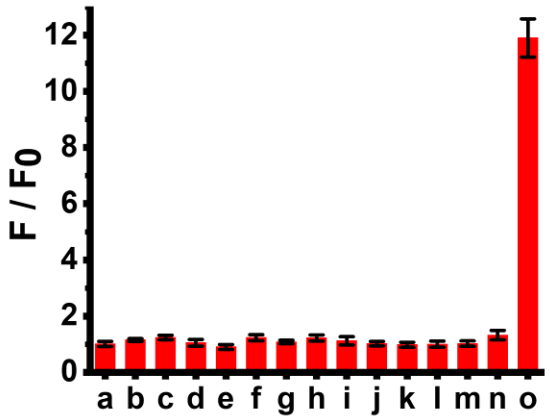

Fig. S11 Fluorescence intensity ratios of BX-BOH@BSA (0.6 mg mL^{-1}, in pH 7.4 PBS containing 5% DMSO) at 938 nm in the presence of various species. a. blank (only BX-BOH@BSA with no other addition), b. Na^+ (1 mM), c. K^+ (1 mM), d. Ca^{2+} (1 mM), e. Mg^{2+} (1 mM), f. glutamic acid (Glu, 1 mM), g. glutathione (GSH, 1 mM), h. cysteine (Cys, 1 mM), i. arginine (Arg, 1 mM), j. tyrosine (Tyr, 1 mM), k. $NaNO_2$ (100 μM), l. NaHS (1 mM), m. NaClO (100 μM), n. $ONOO^-$ (100 μM), o. H_2O_2 (90 μM). Data are means ± SD (n = 3).

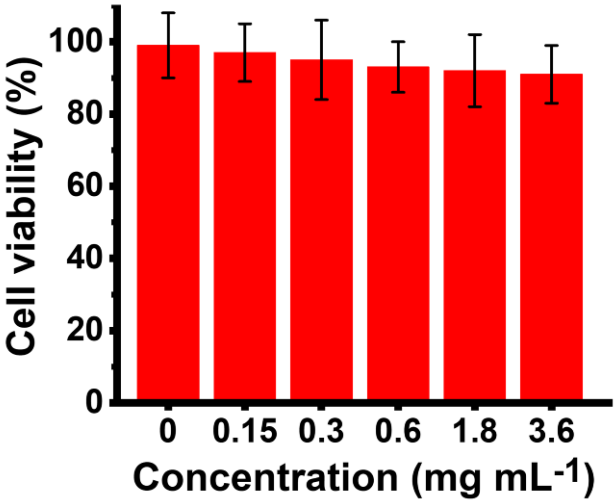

Fig. S12 Cell viability for L929 cells incubated with different concentrations of the nanoprobe BX-BOH@BSA for 24 h by MTT assay. Three independent experiments were conducted for each concentration and eight replicates were performed in each independent experiment. Date represent mean ± SD (n = 3).

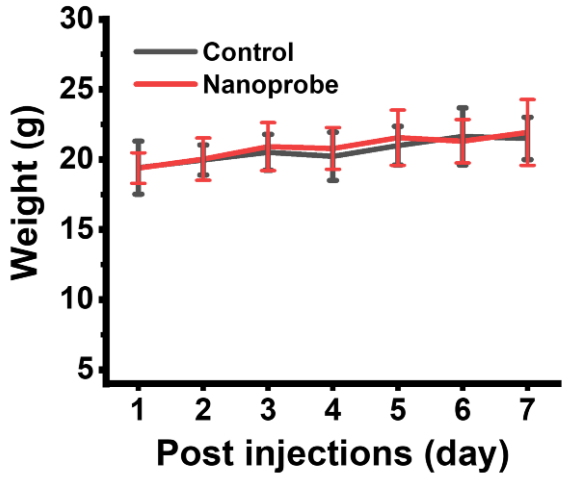

Fig. S13 Body weights for healthy mice i.v. injected with saline (the control) or the nanoprobe BX-BOH@BSA (4 mg kg^{-1}) for 7 days. Date represent mean ± SD (n =5).

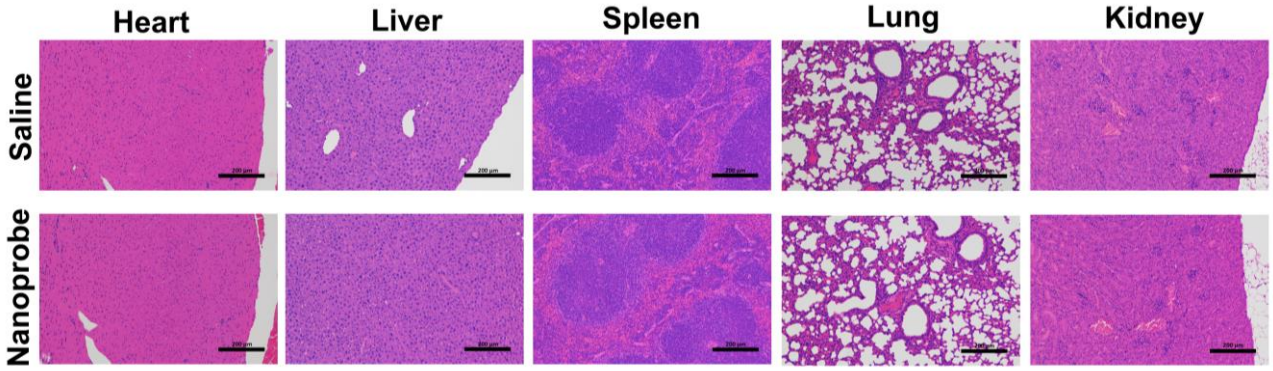

Fig. S14 Histological analysis (H&E staining) for major organs (including hearts, livers, spleens, lungs, and kidneys) from the mice i.v. injected with saline or the nanoprobe BX-BOH@BSA (4 mg kg^{-1}) for 7 days. Scale bar: 200 μm.

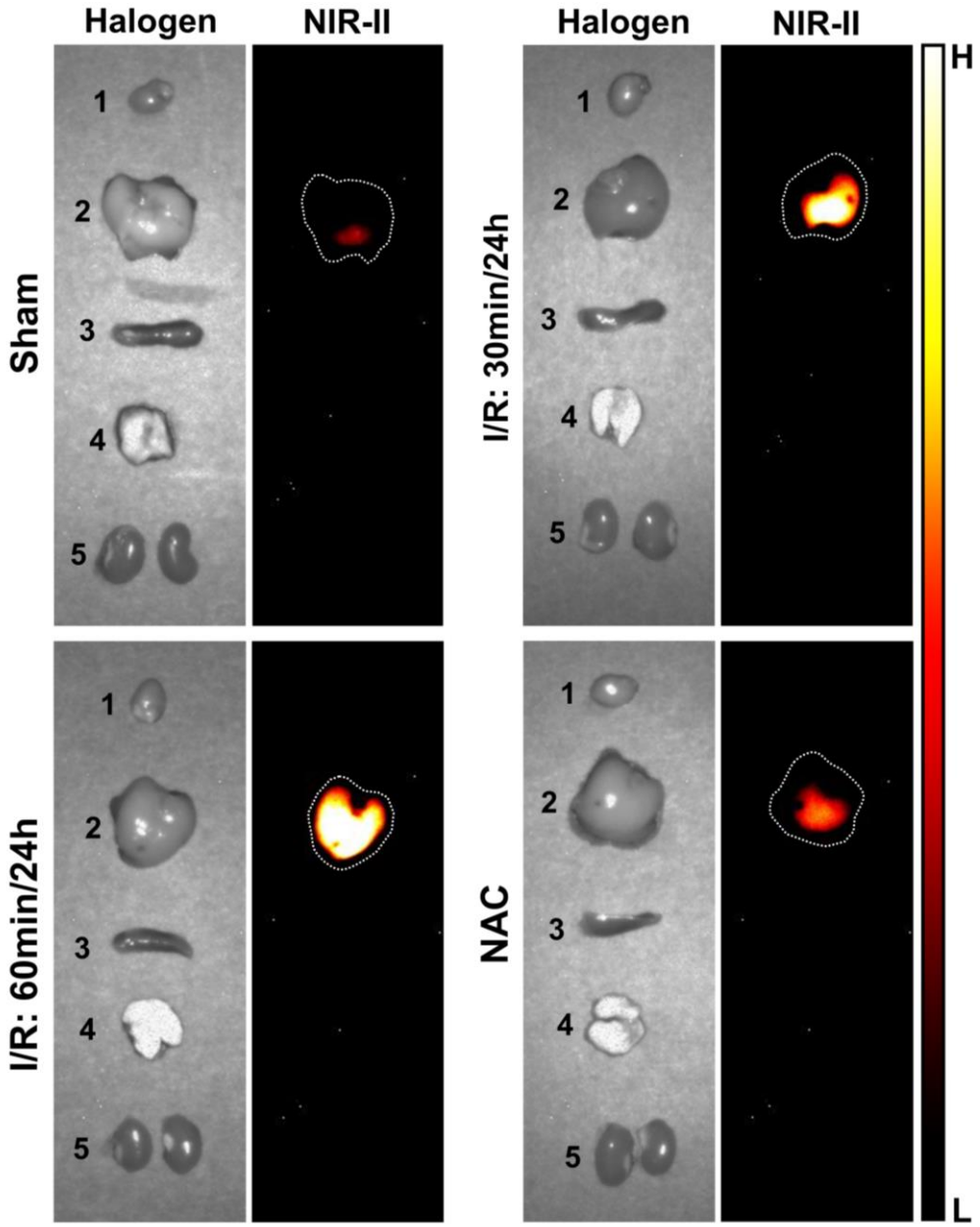

Fig. S15 Representative NIR-II fluorescence images of the organs from different groups of mice at 90 min after intravenous injection of nanoprobe BX-BOH@BSA (4 mg kg^{-1}). Labeling: 1=heart; 2=liver; 3=spleen; 4=lung; 5=kidneys; white dotted lines indicate the liver.

Fig. S16 Photograph of a male mouse in prone posture for indicating the scanning region in MSOT imaging corresponding to Fig. 3A and Fig. S18-21.

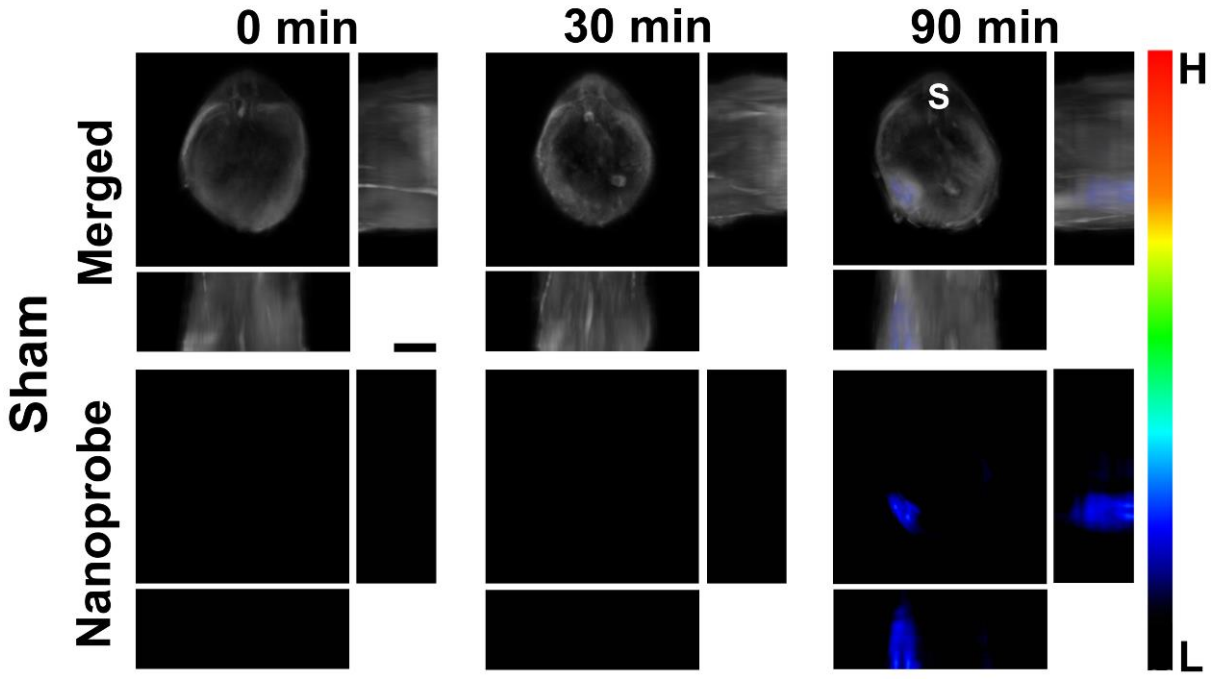

Fig. S17 Orthogonal-view 3D MSOT images of sham group at varied time points upon i.v. injection of nanoprobe BX-BOH@BSA (4 mg kg^{-1}). Upper panel: Overlay of the activated probe's signal with the grayscale single-wavelength (900 nm) background image. Organ labelling: S: Spinal cord. Scale bar: 10 mm.

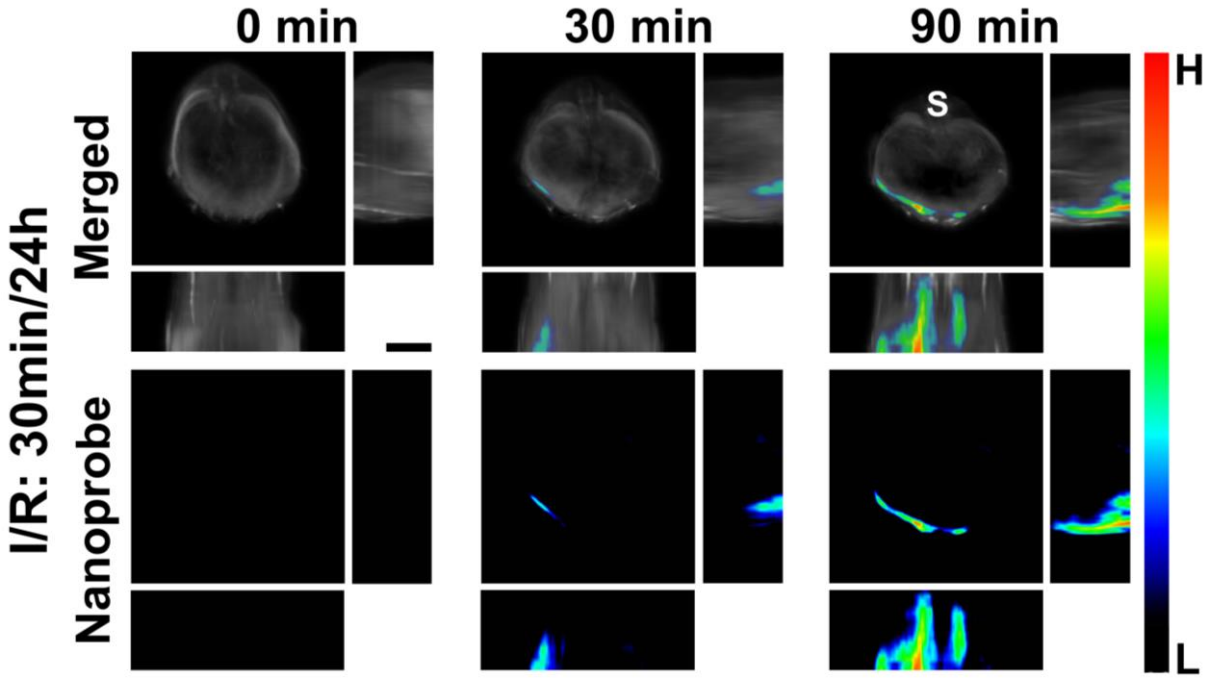

Fig. S18 Orthogonal-view 3D MSOT images of "I/R: 30min/24h" group at varied time points upon i.v. injection of nanoprobe BX-BOH@BSA (4 mg kg^{-1}). Upper panel: Overlay of the activated probe's signal with the grayscale single-wavelength (900 nm) background image. Organ labelling: S: Spinal cord. Scale bar:10 mm.

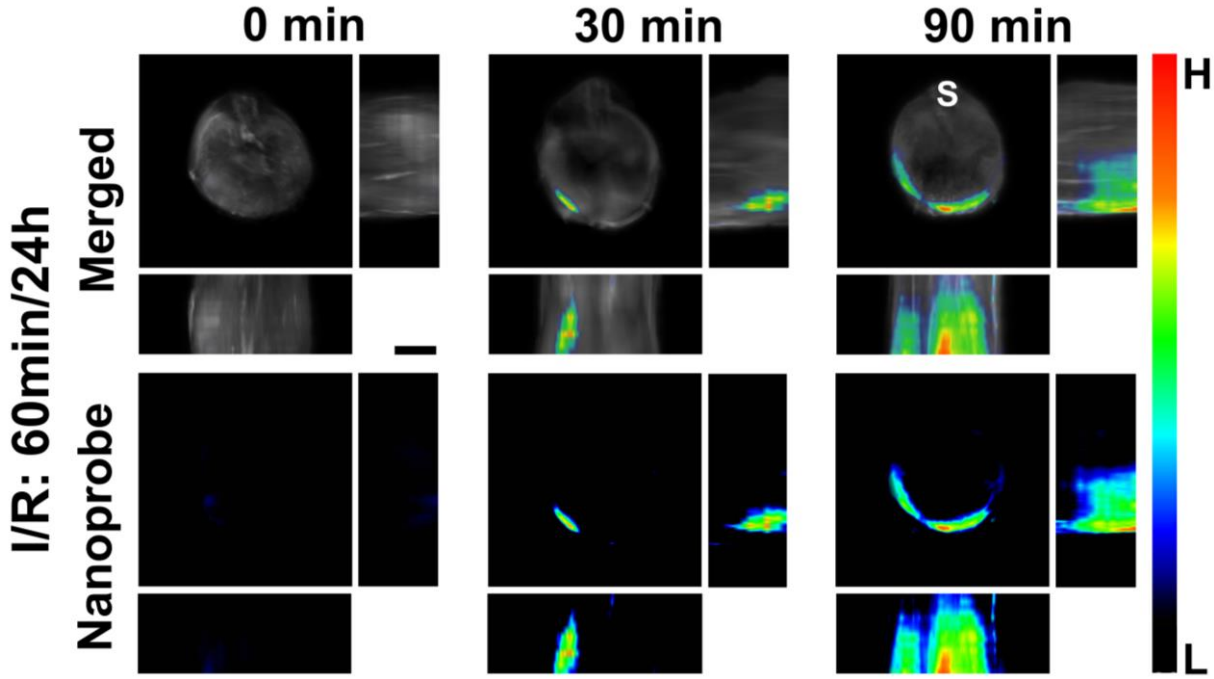

Fig. S19 Orthogonal-view 3D MSOT images of "I/R: 60min/24h" group at varied time points upon i.v. injection of nanoprobe BX-BOH@BSA (4 mg kg^{-1}). Upper panel: Overlay of the activated probe's signal with the grayscale single-wavelength (900 nm) background image. Organ labelling: S: Spinal cord. Scale bar:10 mm.

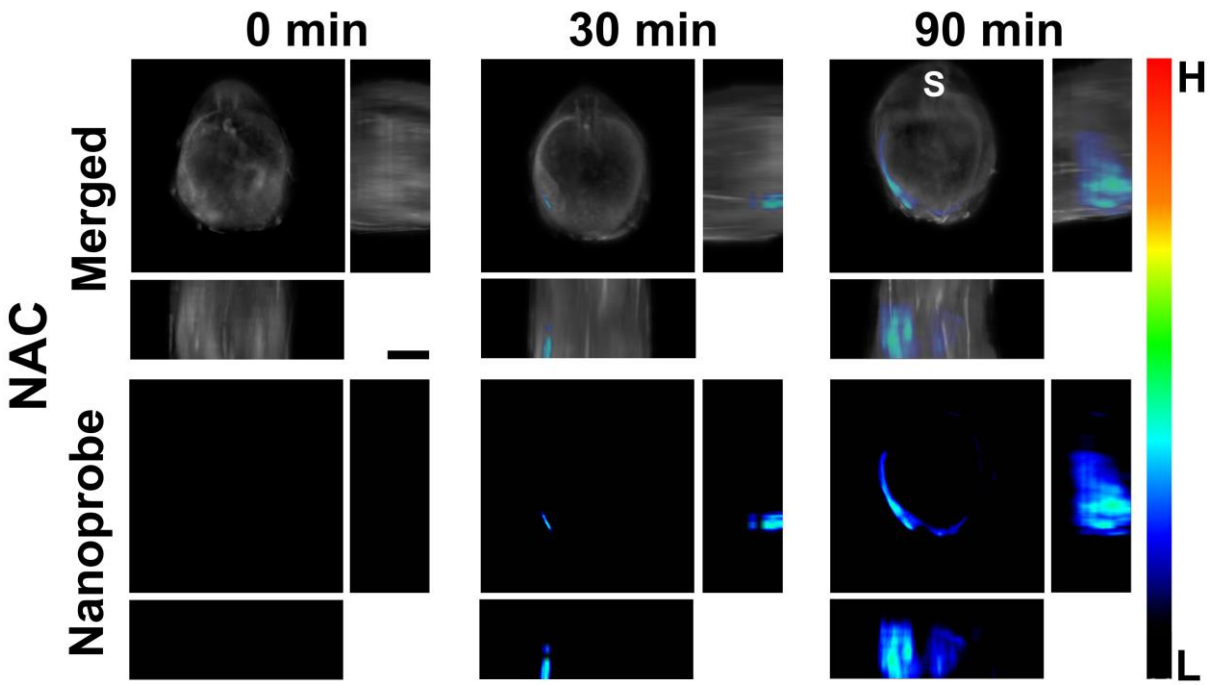

Fig. S20 Orthogonal-view 3D MSOT images of NAC group at varied time points upon i.v. injection of nanoprobe BX-BOH@BSA (4 mg kg^{-1}). Upper panel: Overlay of the activated probe's signal with the grayscale single-wavelength (900 nm) background image. Organ labelling: S: Spinal cord. Scale bar:10 mm.

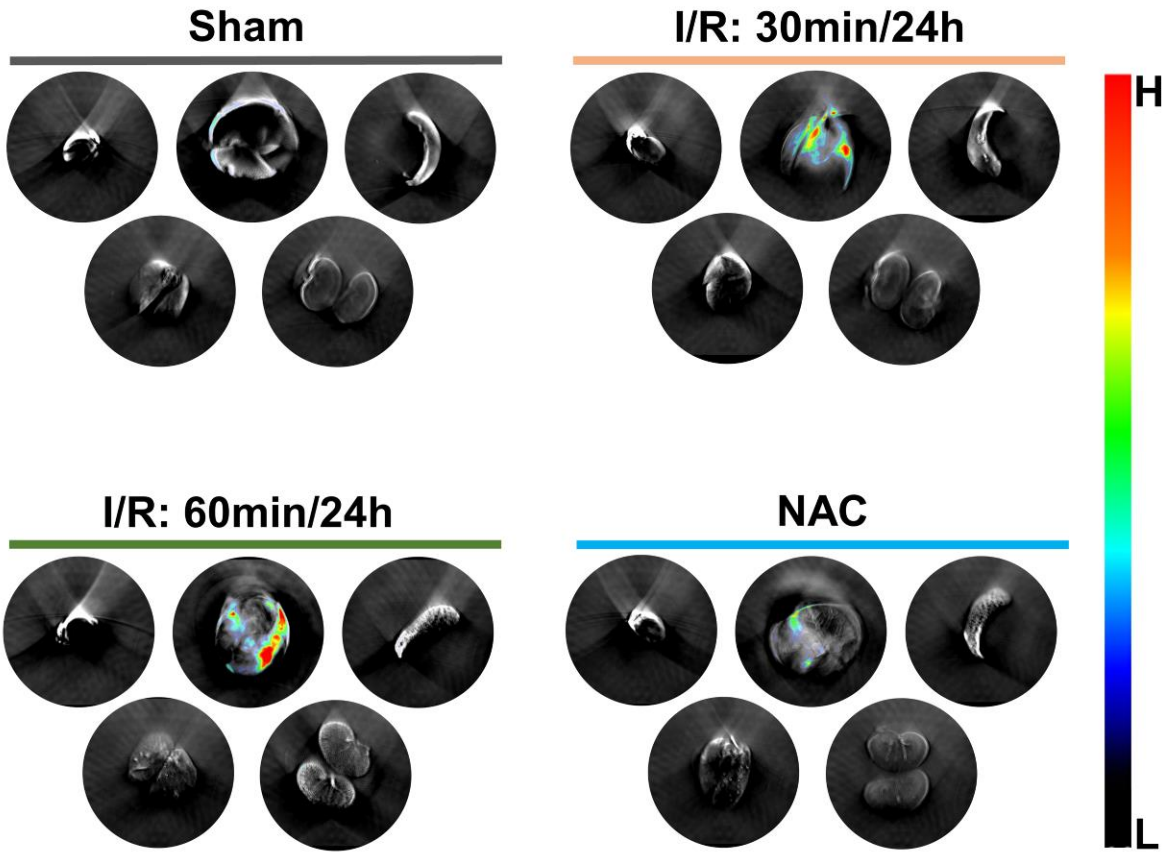

Fig. S21 MOST images of the dissected organs from different groups of mice at 90 min after i.v. injection of nanoprobe BX-BOH@BSA (4 mg kg^{-1}). In each group, from top left to bottom right: heart, liver, spleen, lung, kidney.

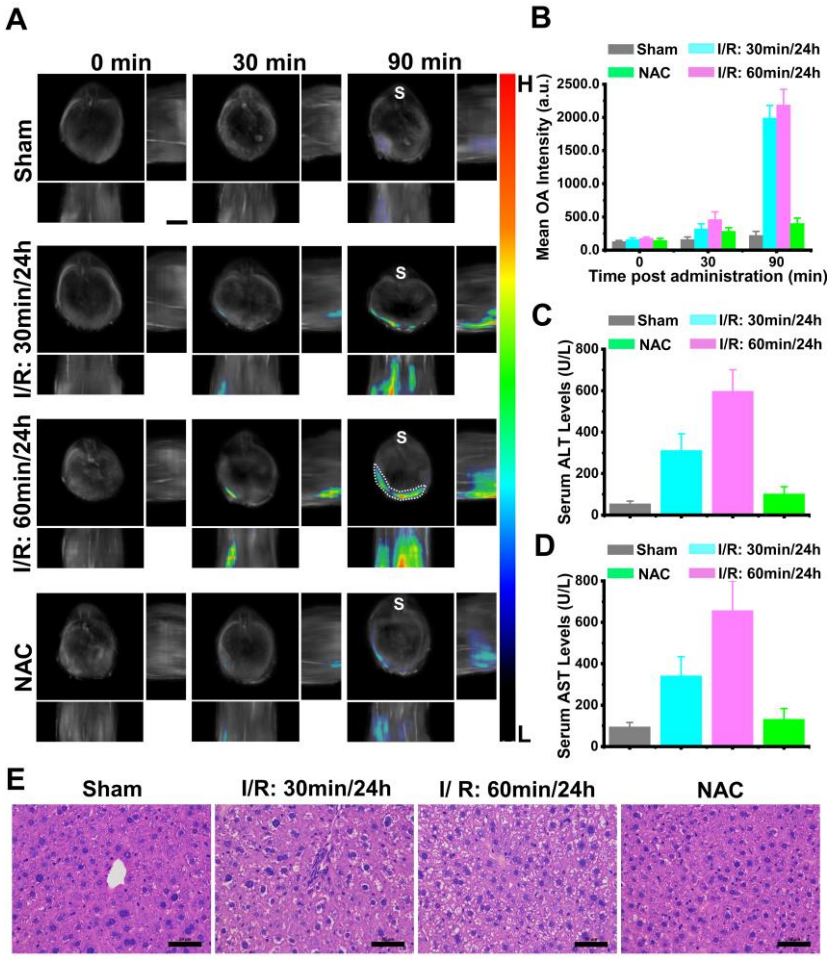

Fig. S22 (A) Mice's orthogonal-view 3D MSOT images at 0, 30, or 90 min upon injection of BX-BOH@BSA (4.0 mg kg^{-1}) via tail vein. Mice were in prone posture. "S" shows spinal cord. The liver region is indicated by white dotted circle. Scale bar: 10 mm. (B) Average MSOT intensities of the VOI (liver region) of different groups at varied time. Date represent mean ± SD (n =5). (C) ALT levels in serum of the mice. (n = 5). (D) AST levels in serum of the mice. (n = 5). (E) H&E staining images of mice's liver sections. Scale bar: 50 μm.

Table S1. DFT calculation data.

	BX-BOH	BX
HOMO-LUMO Energy gap (ev)	-1.70	1.80

Frontier molecular orbital profiles of BX-BOH and BX based on the DFT calculation.

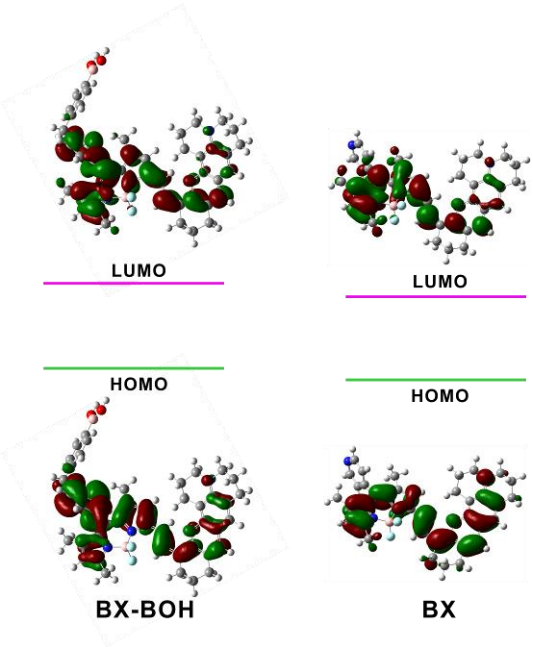

References

[1] Z. Zeng, J. Ouyang, L. Sun, F. Zeng and S. Wu, *Adv. Healthcare Mater.*, 2022, 2201544.
[2] J. Chen, Y. Fang, L. Sun, F. Zeng and S. Wu, *Chem. Commun.*, 2020, **56**, 11102-11105.